Special Issue on Nuclear Science and Technology

ARTICLE

Radiological assessment of groundwater resources: Implications for public health and regulatory compliance

Charles Darwin T. Racadio*[1,2], Jeff Darren G. Valdez[1], Norman DS. Mendoza[1], Raymond J. Sucgang[1], and Mylene G. Cayetano[2]

[1]Philippine Nuclear Research Institute, Department of Science and Technology, Commonwealth Ave., Diliman 1101 Quezon City, Philippines
[2]Institute of Environmental Science and Meteorology, College of Science, University of the Philippines, Diliman, 1101 Quezon City, Philippines

ABSTRACT

This study presents the first systematic radiological assessment of raw groundwater resources in Metro Manila, Philippines, establishing a baseline for public health protection and regulatory compliance. In response to increasing reliance on groundwater following drought-induced surface water shortages, 24 untreated groundwater samples were analyzed for gross alpha, gross beta, and dissolved ^{222}Rn activity concentrations. Gross alpha activities were low (<0.04–0.18 Bq/L), remaining below the Philippine National Standards for Drinking Water (PNSDW) screening level of 0.5 Bq/L. In contrast, gross beta activities ranged from <0.2 to 1.8 Bq/L, with three wells exceeding the national screening level of 1.0 Bq/L. Dissolved ^{222}Rn activities ranged from 2 to 140 Bq/L, with 19 samples exceeding the PNSDW screening level of 11 Bq/L and three exceeding the World Health Organization reference level of 100 Bq/L. Elevated gross beta and ^{222}Rn activities were associated with the volcanic deposits of the Guadalupe Formation and longer groundwater residence times. Age-dependent dose assessment showed that ingestion was the dominant exposure pathway. Mean total annual effective doses (AED_{tot}) were 1.298, 0.801, and 0.727 mSv/y for infants, children, and adults, respectively, all exceeding the WHO individual dose criterion of 0.1 mSv/y. Mean excess lifetime cancer risks were 2.94×10^{-3} for females and 2.63×10^{-3} for males, exceeding the reported global average value of 1.45×10^{-3}. These findings indicate a non-negligible radiological health risk from untreated groundwater consumption and underscore the need for routine radiological monitoring in groundwater management.

INTRODUCTION

Humans are chronically exposed to low-level ionizing radiation from cosmic rays and naturally occurring radionuclides in soil, water, air, food, and biota (Tulchinsky et al. 2023). Dietary intake represents an important pathway of exposure to naturally occurring radionuclides. For instance, consuming potassium-rich foods exposes a person to ^{40}K, a radioactive isotope of potassium. Radionuclides enter food systems through root uptake and atmospheric deposition onto crops, subsequently transferring to animals via contaminated feed and water (BFS 2026; Howard 2021). In hydrogeological settings, uranium-series radionuclides are mobilized into groundwater through prolonged water–rock interactions, contributing to internal exposure when groundwater is abstracted for domestic or agricultural use (Ali et al. 2025). Although doses are generally low, quantifying radionuclide concentrations remains essential for assessing population exposure and radiological risk (Isinkaye et al. 2023; Ofori et al. 2025).

Recognizing the need for regulatory oversight of radioactivity in drinking water, the Philippine Department of Health issued Administrative Order No. 2017-0010, the Philippine National Standards for Drinking Water (PNSDW), harmonized with WHO and U.S. guidelines. The PNSDW applies to all drinking-water providers and includes radiological parameters such as gross alpha and beta activity, ^{222}Rn, and gamma-ray determinations of key radionuclides. The PNSDW establishes screening levels of 0.5 Bq/L for gross alpha activity, 1.0 Bq/L for gross beta activity, and 11.0 Bq/L for ^{222}Rn. These screening levels are conceptually similar to the International Commission on Radiological Protection (ICRP) reference levels, which indicate thresholds at which authorities should consider implementing actions to reduce public exposure, rather than serving as strict regulatory limits. Exceedance of a screening level in raw water does not necessarily

*Corresponding author
Email Address: **ctracadio@pnri.dost.gov.ph**
Date received: 14 May 2026
Dates revised: 30 June 2026; 07 July 2026; 19 July 2026
Date accepted: 21 July 2026
DOI: https://doi.org/10.54645/202619SupEKF-39

KEYWORDS

annual effective dose, gross alpha, gross beta, groundwater quality, radioactivity, ^{222}Rn

indicate that the water is unsafe for consumption. Instead, it serves as a trigger for further investigation, requiring water providers to perform more detailed radiological analyses to identify and quantify the specific radionuclides responsible for the elevated activity concentrations (PNSDW 2017). Conversely, when radioactivity concentrations remain below the screening levels, no additional radiological assessment is generally required, as the water supply is considered acceptable for routine consumption from a radiological protection perspective (WHO 2022).

Gross alpha and beta measurements provide rapid screening, capturing the combined activity of major alpha-emitters (e.g., ^{238}U, ^{226}Ra, ^{210}Po) and beta-emitters (e.g., ^{40}K, ^{228}Ra, ^{210}Pb, ^{234}Th), though weak beta emitters such as ^{3}H and ^{14}C are poorly detected (WHO 2022; Almasoud et al. 2020). When internalized, alpha emitters pose greater hazards due to their high linear energy transfer (Bonotto and Bueno 2008). Previous studies have shown that ^{226}Ra contributes substantially to the ingestion dose (>50%), whereas the contribution of ^{40}K is comparatively minor due to its lower dose conversion factor (Damla et al. 2006; Ho et al. 2020). Accordingly, a conservative assumption is usually adopted whereby gross alpha activity is assumed to be represented by ^{226}Ra, whereas gross beta activity is assumed to be represented by either ^{210}Pb or ^{228}Ra for radiological dose assessment (Ho et al. 2020; Pintilie et al. 2018).

^{222}Rn, a chemically inert decay product of ^{238}U, is tasteless, odorless, and colorless, with a half-life of 3.82 days and potent alpha-emitting properties (Keith et al. 2012). It is the second leading cause of lung cancer after smoking (Lantz et al. 2013; Liu et al. 2025). Radon dissolves into groundwater in contact with uranium-bearing rocks and migrates through fractures into the atmosphere, where it may be captured by rainwater and subsequently deposited on the surface through wet deposition (Mbembe et al. 2021; Mohammed et al. 2026; Livesay et al. 2014; Chen et al. 2018). Household use of radon-rich water releases the gas indoors, exposing occupants through inhalation and ingestion. Inhaled radon progeny, notably polonium isotopes, adhere to lung tissue and emit alpha particles, elevating cancer risk (Eidy et al. 2024; Kashkinbayev et al. 2025; Schwela and Kotzias 2005). Ingestion contributes to gastrointestinal exposure, albeit at lower risk (Barbosa-Lorenzo et al. 2017; Das 2021). Radon has been classified as a Group 1 human carcinogen by the International Agency for Research on Cancer (IARC 1988), a designation reinforced by evidence of its chronic accumulation in poorly ventilated homes. Radon activity in groundwater is strongly influenced by lithology, tectonic activity, and fracture density (Pyuskyulyan et al. 2024). Sustained monitoring of radon concentrations in drinking water, particularly in communities reliant on artesian wells and springs, is critical for early detection of elevated levels and for safeguarding public health.

Metropolitan Manila, officially designated the National Capital Region, serves as the primary metropolitan hub and capital of the Philippines. Historically, the National Water Resources Board (NWRB) sought to protect the region's hydrological integrity by imposing a moratorium on groundwater extraction in 2004. This regulatory action was prompted by evidence that excessive pumping had exacerbated land subsidence, seawater intrusion, and localized flooding (NWRB 2004).

However, the region's heavy reliance on surface water was tested during the severe drought of 2019, when dam levels fell to critical lows, resulting in widespread water shortages. In response, the NWRB lifted the long-standing moratorium, authorizing the drilling of new production wells to supplement the metropolitan supply. Despite this renewed dependence on subterranean sources, the natural radioactivity of groundwater in Metro Manila remains unexplored. While no publicly available local data currently exist on groundwater radioactivity in Metro Manila, a recent study in the neighboring province of Batangas—specifically in municipalities surrounding Taal Volcano—revealed elevated concentrations of ^{222}Rn (Cadungog et al. 2025), highlighting a potential radiological concern that warrants investigation in the capital.

Geology and tectonic setting of Metro Manila

Metro Manila (National Capital Region), the Philippines' largest metropolitan area and seat of government, spans ~636 km² between 14°28'–14°45' N and 120°55'–121°08' E. It comprises 16 cities and one municipality, with a resident population of 13.5 million that swells to 16–21 million daily (PSA 2020).

Morphologically, the region is divided into three units: Coastal Lowland, Central Plateau, and Marikina Valley (Figure 1). These features reflect rapid sedimentation from surrounding highlands through the Late Cretaceous, interspersed with volcanic tuff deposition, followed by tectonic activity during the Late Tertiary–Quaternary. The eastern boundary is marked by basement-ophiolite complexes of Rizal Province (Gervacio 1968; JICA 2010).

The Coastal Lowland comprises flat plains along Manila Bay, including sand bars, tidal flats, the Pasig River delta, and reclaimed lands. Quaternary alluvial deposits reach up to 40 m thick (Miura et al. 2008; Daag et al. 2022), with elevations of 0–5 m in western Mandaluyong and Makati (JICA 2010).

The Central Plateau, underlain by the Guadalupe Formation, covers ~60% of Metro Manila. Elevations range from 20–40 m, rising to 70–100 m in the northwest. Locally termed "adobe," the Guadalupe Formation extends from Quezon City southward to Cavite (Dungca et al. 2018). Drilling records reveal thicknesses of 219–448 m without reaching the base (de la Paz et al. 1989), while estimates suggest 1,300–2,000 m (JICA 1992). Stratigraphy includes the basal Alat Conglomerate and upper Diliman Tuff (Luna et al. 2022), though JICA (1989) subdivided it into six bedrock units. The formation is overlain by alluvium in the coastal areas along Manila Bay and in the Marikina Valley.

The Marikina Valley, on the eastern edge, is a pull-apart basin formed by the West and East Valley Faults (Rimando et al. 2006). Elevations range from 2 m near Laguna de Bay to 30 m at Montalban (JICA 2010). Quaternary alluvium here, associated with the Marikina River floodplain and Laguna de Bay delta, reaches up to 50 m thick (Miura et al. 2008).

Hydrogeologically, sandy alluvium in Manila Bay, Laguna de Bay, and Marikina Valley hosts phreatic aquifers, while the Guadalupe Sedimentary Basin (GSB) of the Guadalupe Formation contains multiple interconnected aquifers of tuffaceous sandstone and conglomerate. Up to five or six aquifers occur within 300 m depth. Groundwater recharge primarily occurs in the northern part of Novaliches, the northern and eastern areas of Montalban, the western portion of the Antipolo Plateau, and the southern terrace composed of lahar deposits contiguous with Tagaytay (JICA 1992). According to the Köppen climate classification, Metro Manila is predominantly characterized by a tropical savanna climate (Aw), with a pronounced dry season generally occurring from January to May and a wetter season from June to December. However, areas in the northeastern part of the metropolitan region, particularly those nearby the Sierra Madre foothills, exhibit characteristics of a tropical monsoon climate (Am), reflecting higher precipitation and a less pronounced dry season. The average rainfall is 2,574.4 mm, with a mean annual temperature and a mean relative humidity of 27.7°C and 78%, respectively (PAGASA 2024).

This study determined the gross alpha and gross beta activity concentrations, as well as the specific ^{222}Rn activity concentrations, in raw groundwater abstracted from production wells across Metro Manila and estimated the annual effective radiation doses resulting from both ingestion and inhalation pathways for infants, children, and adults. This investigation constitutes the first systematic assessment of the radiological quality of groundwater in the National Capital Region, providing a critical baseline dataset for evaluating local radioactivity levels against national and international radiological protection standards. Although the Philippine National Standards for Drinking Water (PNSDW, 2017) require routine monitoring of radioactivity in drinking water supplies, the resulting data are generally not publicly accessible. Consequently, this study represents the first publicly available assessment of groundwater radioactivity in Metro Manila, contributing valuable information for water resource management, public health protection, and future radiological monitoring programs.

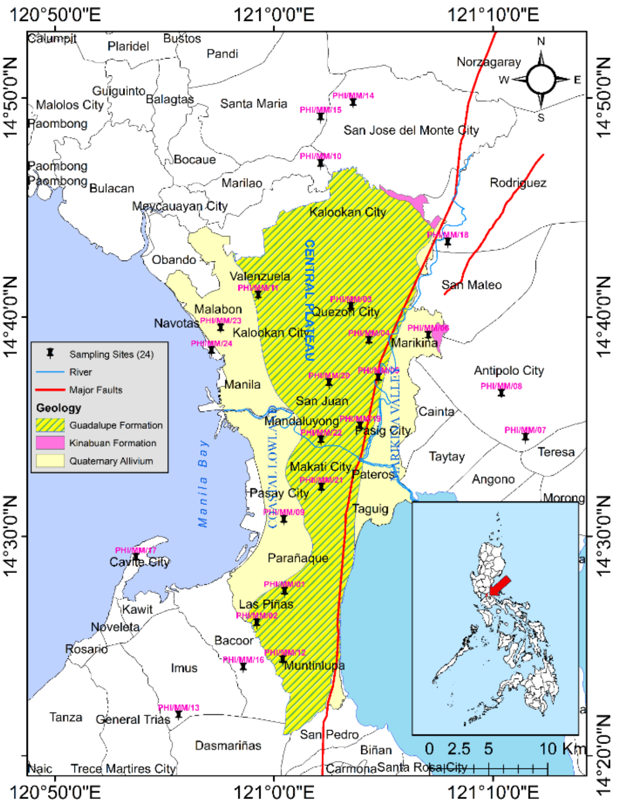

Figure 1: Site map showing the boundaries of Metro Manila, its geology, the adjacent towns, and the sampling sites.

MATERIALS AND METHODS

Sample Collection

Raw groundwater samples were collected from production wells across Metro Manila and its immediate vicinity. These wells are operated by water concessionaires and augment the water supply from dams for domestic and commercial use. A total of 24 groundwater samples were obtained for analysis (Figure 1). The number of samples was based on existing and functioning production wells in the study area.

Prior to sampling, wells were purged until field parameters stabilized to ensure representative aquifer conditions. Stabilization was confirmed when specific conductivity, pH, and temperature showed minimal variation between consecutive measurements. Field parameters were measured in situ using calibrated portable meters. Bicarbonate concentration was also measured in-situ using a Hach digital titration with a 1.6 N H_2SO_4 cartridge. The groundwater samples were collected directly from the well discharge point. For tritium measurement, samples were collected in 1-L high-density polyethylene (HDPE) bottles that were filled to the brim, ensuring no airspace or bubbles were present. For gross alpha and beta analyses, samples were collected in pre-cleaned 1-L HDPE bottles and preserved with HCl to about pH 2. For ^{222}Rn analysis, water samples were collected from a non-aerated faucet using a delivery tube. The tube outlet was positioned at the bottom of a 1-L amber glass bottle placed inside a 2-L beaker, allowing the bottle to be filled from the bottom while minimizing agitation and potential ^{222}Rn loss. Water was allowed to flow gently through the tube until the bottle overflowed into the beaker, and flushing was continued until approximately 2–3 bottle volumes had been displaced to minimize atmospheric contamination and ensure that residual line water was replaced with representative aquifer groundwater. The bottle was then capped while submerged to avoid trapping air. After sealing, the bottle was inverted and inspected for air bubbles; if any bubbles were observed, the sampling procedure was repeated. The date and time of collection were recorded for decay correction purposes. Samples were immediately placed in ice-filled insulated coolers and transported to the laboratory, where they were stored at 4 °C until analysis

Measurement of Tritium Concentrations

Tritium concentrations in the samples were measured at the International Atomic Energy Agency Isotope Hydrology Laboratory by the ^{3}He ingrowth method following the method detailed in Mabry et al. (2022).

Briefly, the analysis began by thoroughly degassing a water sample under vacuum to eliminate all pre-existing helium isotopes. After the degassing was complete and the time was recorded as t_0, the sample was stored in a leak-tight stainless-steel container for approximately one to three months. During this storage window, tritiogenic ^{3}He accumulated as a direct product of radioactive tritium decay. Following the accumulation phase, the sample was agitated with a magnetic stirrer, and the accumulated gas was transferred via a water vapor stream through a series of cryogenic and charcoal traps designed to separate and fully purify the helium fraction. Subsequently, the pure helium was released into a highly sensitive mass spectrometer under static vacuum. The mass spectrometer's sensitivity was calibrated using a pure ^{3}He spike running standard, allowing the final tritium concentration at the time of sampling to be mathematically calculated from the measured volume of tritiogenic ^{3}He.

Optimization of Liquid Scintillation Counting Parameters

Prior to analysis, the PerkinElmer Tri-Carb 3180 TR/SL liquid scintillation counter was optimized for the measurement of alpha and beta activities. The calibration of the detector was carried out using ^{241}Am ($t_{1/2}$: 432 y; α % probability: 99.9%; Emax: 5.5 MeV) and ^{36}Cl ($t_{1/2}$: 3 x 10^5 y; β % probability: 99%; Emax: 710 keV) standards from the National Institute of Standards and Technology (NIST), USA. Solutions for each radionuclide were prepared from the certified reference standards. A 1-mL aliquot from the prepared solutions was mixed with 19 mL of Revvity (formerly PerkinElmer) Ultima Gold AB (P/N: 6013309) in a 20-mL low-potassium glass vial to achieve a target count rate of approximately 5,000 counts per minute (cpm). The standards were prepared using the same type of scintillant, sample-scintillant ratio, volume, and vials as the samples to be counted.

The instrument discriminator, which differentiates alpha and beta events based on the decay characteristics of their scintillation pulses, was optimized using the Pulse Shape Analysis (PSA) feature of the liquid scintillation counter. The optimum PSA setting was established by measuring the prepared alpha and beta standards to achieve maximum alpha/beta discrimination while minimizing event misclassification. The optimized discriminator setting was determined to be at 128 (Figure 2). The instrument was configured to acquire data over the full counting window.

Figure 2: The determined optimized discriminator setting of the PerkinElmer Tricarb 3180 TR/SL.

Gross Alpha and Beta Activity Concentration Analysis

Gross alpha and beta activity analyses were conducted within 5 days of sample collection, following the in-house analytical method developed and optimized by the Nuclear Analytical Techniques Application Section of the Philippine Nuclear Research Institute. The full method is detailed in Sucgang et al. (2012) and Sucgang et al. (2023).

Briefly, a 100-mL aliquot of the groundwater sample was pipetted into a labeled beaker and evaporated to dryness on a hot plate set to 80°C. After drying, 1 mL of 0.1 M HCl was added to the beaker to dissolve the residues, and the mixture was pipetted into a 20-mL low-potassium glass vial. 19 mL of Revvity (formerly PerkinElmer) Ultima Gold AB scintillant was added, and the mixture was shaken. A procedural blank was prepared using "dead water" (i.e., deionized water that had been stored for at least one month) and processed following the same preparation and counting procedures as the samples. This blank was used to determine background contributions and to verify the absence of contamination during sample preparation and analysis. The prepared samples and blank were allowed to equilibrate for at least 72 h prior to analysis.

The prepared scintillation samples and three quality control standards of known gross alpha and beta activities (i.e., IAEA-TERC-2022-01/02) were analyzed for gross alpha (α) and gross beta (β) activities using a PerkinElmer Tri-Carb 3180 TR/SL liquid scintillation counter. Prepared ^{241}Am and ^{36}Cl standards were analyzed with each batch to determine alpha and beta counting efficiencies, respectively. Samples were counted for 6 h in a single counting cycle to maximize counting statistics and minimize detection limits. All analyses were performed in duplicate to evaluate analytical precision.

The alpha and beta specific activities were calculated using the equation:

$$A_{(\alpha/\beta)} = \frac{cpm_{spl} - cpm_{blk}}{\varepsilon \; x \left(\frac{60\,s}{min}\right) x \; V_{spl}} \quad (1)$$

where:

- $A_{(\alpha/\beta)}$ = gross alpha or beta activity in Bq/L
- cpm_{spl} = instrument count of sample in counts per minute
- cpm_{blk} = instrument count of blank in counts per minute
- $\varepsilon\ (Efficiency) = \frac{cpm_{std} - cpm_{blk}}{dpm)_{std}}$

  where:

  ➢ AA dpm_{std} = activity of ^{241}Am or ^{36}Cl standard in disintegrations per minute
- V_{spl} = volume of sample in L

The Lower Limit of Detection (LLD) for alpha and beta measurements was calculated by the equation:

$$LLD = \frac{4.65 * \sqrt{cpm_{blk}}}{\left(\frac{60\,s}{min}\right) * \varepsilon * V_{spl}} \quad (2)$$

where:

- 4.65 = correction factor accounting for 5% probability of making a Type I and Type II error (Currie 1968)

The combined standard uncertainty associated with the calculated activity was determined using the equation:

$$Unc_{\alpha/\beta} = \sqrt{\left(\frac{unc\ net\ cpm}{net\ cpm}\right)^2 + \left(\frac{unc\ Eff}{Eff}\right)^2 + \left(\frac{unc\ vol}{vol}\right)^2} \quad (3)$$

where:

- $\text{Unc net cpm} = \sqrt{(unc\ cpm_{\ blk})^2 + (unc\ cpm_{\ spl})^2} \quad (4)$

  where:

  ➢ $Unc\ cpm_{blk/spl} = cpm\ x\ counting\ error\ factor$

- $\text{Unc Eff} = \sqrt{\left(\frac{unc\ cpm_{std}}{cpm_{std}}\right)^2 + \left(\frac{unc\ dpm_{std}}{dpm_{std}}\right)^2} \quad (5)$

  where:

  ➢ $Unc\ dpm_{std} = dpm_{std}\ x \sqrt{\left(\frac{unc\ vol}{vol}\right)^2 + \left(\frac{unc\ half-life}{half\ life}\right)^2} \quad (6)$

- $\text{Unc vol} = \frac{specific\ tolerance\ of\ volumetric\ glasswares}{\sqrt{6}} \quad (7)$

^{222}Rn Activity Concentration Analysis

The ^{222}Rn activity analysis was performed within 24 h of sampling, using an in-house method developed and optimized by the Nuclear Analytical Techniques Application Section. The method is based on the 7500-Rn B. Liquid Scintillation Method of the Standard Methods for the Examination of Water and Wastewater (APHA 2023).

Briefly, a 10-mL aliquot of the groundwater sample was carefully pipetted into a 20 mL plastic vial, and 10 mL of scintillant was added; the mixture was then shaken vigorously and allowed to equilibrate for 3 hours. A blank sample was prepared by the same method using sonicated ultrapure water to ensure the absence of radon. A calibration standard was prepared by diluting a ^{226}Ra standard solution in water and allowing it to age for at least 25 days to establish secular equilibrium with the generated ^{222}Rn. The resulting standard was prepared to produce a target count rate of approximately 5,000 cpm during liquid scintillation counting. Additionally, a quality standard of known ^{222}Rn activity concentration was included in each run.

The prepared samples, standard, and blank were counted using a PerkinElmer Tri-Carb 3180 TR/SL liquid scintillation counter for a total of 1 hour, divided into two cycles. ^{222}Rn activity and uncertainties were calculated using Eqs. 1–7. However, the activity must be corrected due to the short half-life of ^{222}Rn. The activity was corrected to the time and date of sampling using the formula:

$$N_{t1} = N_{t2}e^{\lambda t} \quad (8)$$

where:

- N_{t1} = activity concentration at the time of sampling (t_1)
- N_{t2} = activity concentration at the time of counting (t_2)
- $\lambda = \frac{\ln(2)}{T_{1/2}}$, where $T_{1/2} = 3.82$ days
- t = elapsed time from t_1 to t_2

Estimation of annual effective doses (AED) for gross alpha and beta, and ^{222}Rn by ingestion and inhalation

To calculate the annual effective dose by ingestion (AED_{ing}) from the gross alpha and beta, and ^{222}Rn activity concentrations in water, the activities (Bq/L) were converted into radiation dose (Sv/y) using the equation:

$$AED_{(\alpha/\beta/Rn),ing}\ (Sv/y) = C \ x \ IR \ x \ DCF \quad (9)$$

where:

- C = Activity concentration (Bq/L)
- IR = Annual ingestion rate of water (L/year)
- DCF = Dose conversion factor (Sv/Bq)

The World Health Organization (WHO, 2022) estimates the average annual water intake of adults at 2 L/day (approximately 730 L/year). The United Nations Scientific Committee on the Effects of Atomic Radiation (UNSCEAR 2008) report provides age-specific annual water intake rates of 150 L/year for infants and 350 L/year for children.

For conservative purposes, gross alpha was assumed to be represented by ^{226}Ra and gross beta by ^{210}Pb. Dose conversion factors (DCFs) for ^{226}Ra were used to calculate the annual effective dose due to ingestion (AED_{ing}) from gross alpha activity, while the DCFs for ^{210}Pb were applied for the calculation of AED_{ing} from gross beta activity. The AED_{ing} from ^{222}Rn was calculated separately using the corresponding DCFs for ^{222}Rn. Table 1 summarizes the age-specific annual water consumption rates and the radionuclide-specific DCFs applied for each age group.

Table 1: Age-specific annual water consumption rates and dose coefficients of different radionuclides.

Age Groups	Annual Ingestion rate of water (L/y)[1]	Dose Conversion Factor (Sv/Bq)		
		^{226}Ra[2]	^{210}Pb[2]	^{222}Rn[3]
Adult (≥ 17 y)	730	2.8×10^{-7}	6.9×10^{-7}	1×10^{-8}
Children (10 y)	350	8.0×10^{-7}	1.9×10^{-6}	2×10^{-8}
Infant (< 1 y)	150	4.7×10^{-6}	8.4×10^{-6}	7×10^{-8}

[1]WHO 2022; UNSCEAR 2008
[2]ICRP 2012
[3]Cadungog et al. 2025; Ezzulddin and Mansour 2017

The annual effective dose due to inhalation (AED_{inh}) of ^{222}Rn that escaped from the drinking water into indoor air was estimated using the equation (UNSCEAR 2000; Elzain et al. 2024):

$$AED_{Rn,inh}(Sv/y) = C_{RnW} \ x \ O \ x \ E_f \ x \ R \ x \ D \quad (10)$$

where:

- C_{RnW} = Activity of ^{222}Rn in water in Bq/m^3
- O = Average indoor occupancy time per individual (7000 h/y; UNSCEAR, 2000)
- E_f = Equilibrium factor equal to 0.4 (UNSCEAR, 2000)
- R = Ratio of radon in air to water equal to 10^{-4} (UNSCEAR, 2000)
- D = Dose conversion factor equal to 9×10^{-9} Sv/h/(Bq/m^3) (UNSCEAR, 2000)

In addition to the radiation dose received through ingestion and inhalation of radon, an additional internal dose may result from the transfer of dissolved radon into the bloodstream following inhalation. The annual effective dose attributable to this component was estimated using the following equation (UNSCEAR 2000; Pyuskyulyan et al. 2024):

$$AED_{Rn,di}(Sv/y) = C_{RnW} \ x \ O \ x \ R \ x \ DCF_{di} \quad (11)$$

where:

- $AED_{Rn,di}$ = Annual effective dose due to radon dissolved in blood via inhalation
- C_{RnW} = Activity of ^{222}Rn in water in Bq/m^3
- O = Average indoor occupancy time per individual (7000 h/y; UNSCEAR, 2000)
- R = Ratio of radon in air to water equal to 10^{-4} (UNSCEAR, 2000)
- DCF_{di} = 0.17×10^{-9} Sv/h/(Bq/m^3) (UNSCEAR, 2000)

The total annual effective dose (AED) was calculated as the sum of: (1) the annual effective dose due to ingestion of drinking water containing gross alpha and gross beta emitters and dissolved ^{222}Rn, (2) the annual effective dose due to inhalation of ^{222}Rn released into indoor air from water use, and (3) the annual effective dose due to radon dissolved in blood via inhalation.

$$AED_{tot} = AED_{\alpha,ing} + AED_{\beta,ing} + AED_{Rn,ing} + AED_{Rn,inh} + AED_{Rn,di} \quad \text{a xx} \quad (12)$$

where:

- $AED_{\alpha,ing}$ = dose from ingestion of gross alpha emitters
- $AED_{\beta,ing}$ = dose from ingestion of gross beta emitters
- $AED_{Rn,ing}$ = dose from ingestion of dissolved ^{222}Rn
- $AED_{Rn,inh}$ = dose from inhalation of ^{222}Rn released from water
- $AED_{Rn,di}$ = dose due to radon dissolved in blood via inhalation

Lifetime excess cancer risk

The excess lifetime cancer risk (ELCR) was used to assess the potential carcinogenic risk to the local population arising from exposure to radioactivity in water. It estimates the incremental probability of developing cancer over a lifetime as a consequence of chronic exposure to radionuclides through water consumption. According to the WHO (2026) data from 2000 to 2021, the average life expectancy of Filipinos is 73.6 for females and 65.7 for males. The ELCR is calculated using the formula (Shouop et al. 2026):

$$ELCR = AED_{tot} \ x \ D_L \ x \ RF \quad (13)$$

where:

- D_L = average life expectancy in years
- RF = stochastic risk factor (5.5×10^{-2}/Sv; UNSCEAR 2000; WHO 2011)

RESULTS AND DISCUSSION

Gross Alpha, Gross Beta Activity, and ^{222}Rn Activity Concentrations

Gross alpha activity was detected above the lower limit of detection (LLD = 0.04 Bq/L) in 63% (15 of 24) of the groundwater samples (Table 2). Concentrations ranged from <0.04 to 0.18 Bq/L, with a mean of 0.078 ± 0.059 Bq/L and a median of 0.055 Bq/L. To prevent statistical bias and artificial truncation of variance, non-detect values (<LLD) were imputed using the LLD/√2 substitution method rather than zero-substitution (Hornung and Reed 1990). This approach is optimized for naturally skewed, log-normal biological or environmental concentrations, as it provides a robust mathematical approximation of the geometric mean and geometric standard deviation of the censored data segment (Hornung and Reed 1990; Lubin et al. 2004). Notably, all samples remained well below the 0.5 Bq/L screening level mandated by the Philippine National Standards for Drinking Water (PNSDW 2017).

In contrast, gross beta activity exceeded its LLD (0.2 Bq/L) in 14 samples, ranging from <0.2 to 1.8 Bq/L (mean: 0.51 ± 0.50 Bq/L; median: 0.25 Bq/L). Three samples exceeded the 1.0 Bq/L screening level: two from the southern sector of Metro Manila (1.8 Bq/L) and one from Makati City (1.1 Bq/L). Relatively high gross beta activity concentrations were measured in water samples collected along the Guadalupe Formation, which extends south towards Tagaytay City in Cavite Province, compared to samples from Marikina Valley and Coastal Lowland (Figure 3). The Guadalupe Formation is composed largely of ancient volcanic ash, tuff, and magmatic debris, which are naturally rich in radioactive elements such as ^{40}K and trace products of uranium and thorium. As groundwater interacts with and weathers these volcanic minerals, beta-emitting isotopes are leached into solution. In contrast, the sediments in the Marikina Valley and Coastal Lowland have either already been thoroughly leached of these highly soluble radioactive elements over millennia of river transport, or they lack the inherent volcanic mineral composition required to elevate beta activity. Measured gross alpha and beta activity concentrations in Metro Manila are higher than in Serbia and Albania but lower than in most countries (Table 3).

Table 2: Gross alpha, gross beta, and 222Rn activity concentrations of the groundwater samples with corresponding uncertainties.

Sample Code	Location	pH	EC	^{3}H	Gross Alpha (Bq/L)		Gross Beta (Bq/L)		^{222}Rn (Bq/L)	
			µS/cm	TU	A_α	Unc.**	A_β	Unc.**	A_{222Rn}	Unc.**
PHI/MM/01	Parañaque City	8.5	664	0.02	0.18	0.04	0.70	0.1	38	4
PHI/MM/02	Las Piñas City	8.1	790	0.19	0.18	0.04	0.50	0.1	19	3
PHI/MM/03	Quezon City	8.3	426	0.02	<0.04		0.20	0.1	23	3
PHI/MM/04	Quezon City	8.4	415	0.02	0.18	0.04	<0.20		86	6
PHI/MM/05	Marikina City	8.4	523	0.13	0.04	0.03	0.50	0.2	24	3
PHI/MM/06	Marikina City	7.9	400	0.45	0.06	0.03	<0.20		15	3
PHI/MM/07	Antipolo City, Rizal	7.5	289	0.56	0.08	0.03	<0.20		6	2
PHI/MM/08	Antipolo City, Rizal	7.9	230	0.53	0.11	0.03	<0.20		2	2
PHI/MM/09	Pasay City	8.3	3,940	0.13	0.06	0.03	0.60	0.2	34	4
PHI/MM/10	Caloocan City	8.3	476	0.02	0.05	0.03	<0.20		8	2
PHI/MM/11	Valenzuela City	8	339	0.39	0.04	0.03	<0.20		14	3
PHI/MM/12	Las Piñas City	8.3	557	0.02	0.09	0.03	<0.20		107	6
PHI/MM/13	Imus, Cavite	8.3	506	0.02	0.12	0.03	<0.20		115	7
PHI/MM/14	San Jose Del Monte, Bulacan	8.3	513	0.18	0.18	0.05	0.20	0.1	8	2
PHI/MM/15	San Jose Del Monte, Bulacan	8.1	535	0.15	<0.05		0.70	0.1	11	2
PHI/MM/16	Bacoor, Cavite	8.1	545	0.02	<0.05		1.80	0.1	21	3
PHI/MM/17	Cavite City, Cavite	8.2	717	0.02	0.18	0.05	1.80	0.1	98	6
PHI/MM/18	Rodriguez, Rizal	7.6	583	0.13	0.04		1.00	0.2	17	3
PHI/MM/19	Pasig City	7.8	445	0.14	<0.04		0.80	0.2	33	4
PHI/MM/20	Quezon City	7.8	413	0.25	<0.04		0.60	0.2	37	4
PHI/MM/21	Makati City	7.8	552	0.11	<0.04		1.10	0.2	91	6
PHI/MM/22	Mandaluyong City	7.9	444	0.02	0.06	0.04	0.30	0.1	93	6
PHI/MM/23	Malabon City	7.9	443	0.02	<0.04		<0.20		140	11
PHI/MM/24	Navotas City	7.7	450	0.02	<0.04		<0.20		58	11
Mean ± SD*					**0.078 ± 0.059**		**0.509 ± 0.497**		**47.0 ± 43.6**	
Median*					**0.055**		**0.25**		**35.5**	
Range					**<0.04 – 0.18**		**<0.2 – 1.8**		**2 - 140**	

*Values for "<LLD" are treated as LLD/√2
** Unc. = uncertainty calculated by error propagation

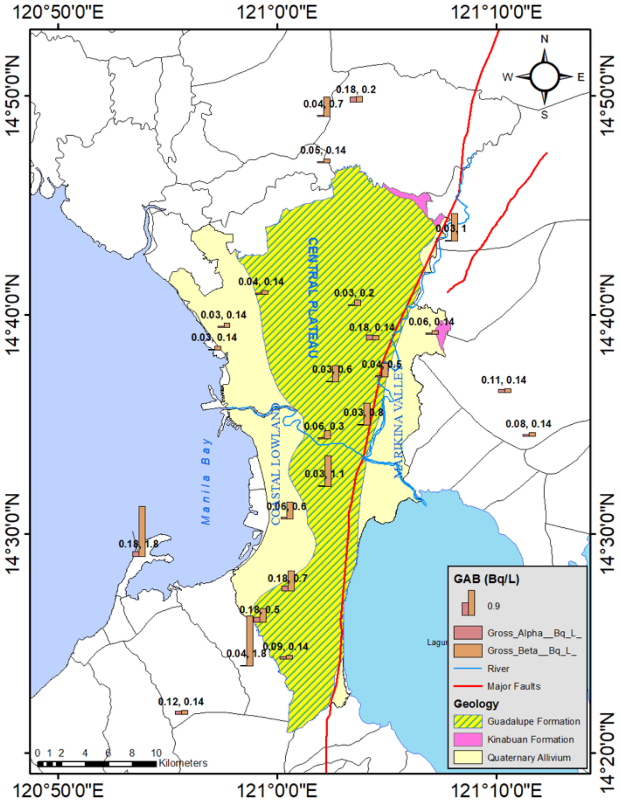

Figure 3: Spatial distribution of measured gross alpha and gross beta activity concentrations in groundwater samples. Each bar is labeled with the corresponding gross alpha and gross beta activity concentrations, separated by a comma.

Table 3: Comparison of the gross alpha and beta activity concentrations determined in groundwater samples with those reported in other countries.

Region/Country	A_α (Bq/L)		A_β (Bq/L)		References
	Mean	Range	Mean	Range	
Albania	–	0.01 – 0.126	–	0.09 – 0.884	Cfarku et al. 2014
Balaton, Hungary	0.189	0.035 – 1.749	0.209	0.033 – 2.105	Jobbágy et al. 2011
Brazil	–	<0.001 – 0.428	–	0.08 – 5.22	Bonotto 2019
China	0.029	0.000498 – 0.49	0.075	0.005 – 1.26	Sang et al. 2021
Enugu State, Nigeria	0.2174	0.015 – 0.546	32.105	2.153 – 122.663	Avwiri et al. 2016
Galati, Romania	0.022	<0.06 – 0.852	0.076	<0.025 – 0.435	Pintilie et al. 2016
Italy	–	<0.008 – 0.186	–	<0.048 – 0.150	Forte et al. 2007
Metro Manila, Philippines	0.078	<0.04 – 0.18	0.51	<0.2 – 1.8	This study
Nevsehir, Türkiye	0.192	0.08 – 0.380	0.579	0.120 – 3.47	Turhan et al. 2013
Northern Saudi Arabia	3.51	0.96 – 8.97	3.48	1.26 – 6.63	Almasoud et al. 2020
Serbia	–	0.001 – 0.013	–	0.041 – 0.173	Jankovic et al. 2012
Southern Vietnam	0.183	0.024 – 0.748	0.15	0.027 – 0.632	Ho et al. 2020

Dissolved ^{222}Rn activity concentrations ranged from 2 to 140 Bq/L, with mean and median values of 45.75 ± 41.3 Bq/L and 28.5 Bq/L, respectively (Table 2; Figure 4). Nineteen samples exceeded the Philippine screening level of 11 Bq/L, eight exceeded the UNSCEAR (2000) reference level of 40 Bq/L, and three exceeded the WHO (2022) reference value of 100 Bq/L. While relatively high ^{222}Rn activity concentrations can be observed from samples along the Guadalupe Formation, high ^{222}Rn activity concentrations were also observed in samples along the Coastal Lowland, signifying that other factors, beyond local geology, contribute to elevated radon concentrations. As the Coastal Lowland is a regional discharge zone, groundwater from higher regions flows downhill and accumulates in this basin. This slow-moving, deeply circulating groundwater has had a very long time to absorb radon along its journey before pooling in the coastal area. Additionally, coastal areas often have thick, impermeable layers of marine clay overlying the water. The low-permeability clay layer functions as an effective confining unit that restricts the upward migration of radon gas. As a result, radon is retained within the saturated zone, promoting its dissolution into groundwater rather than allowing its diffusion and escape to the atmosphere.

Compared with other volcanic aquifer systems worldwide, the observed ^{222}Rn concentrations in Metro Manila were elevated but remain within reported international ranges (Table 4). For example, groundwater from the Batangas volcanic area in the Philippines has ^{222}Rn activity concentrations of 4–51 Bq/L (Cadungog et al. 2025), while groundwater from volcanic regions in Italy ranges 1.00–37.23 Bq/L (Iannone et al. 2024). These comparisons indicate that Metro Manila groundwater exhibits moderate-to-high radon enrichment consistent with fractured volcanic lithologies and prolonged water–rock interaction.

Pearson correlation analysis was performed to determine the relationship between gross alpha, gross beta, 222Rn activity concentrations, bicarbonate concentrations, electrical conductivity, pH, and tritium concentration (Table 5). Using the conventional significance threshold of $p < 0.05$, only four correlations were statistically significant in the dataset: gross alpha vs. pH, gross beta vs. bicarbonate, gross beta vs. electrical conductivity, and 222Rn vs tritium. The remaining correlations were not statistically significant, even though some have moderate correlation coefficients.

Gross alpha and gross beta activity concentrations vary independently, indicating that the radionuclides contributing to each are likely different and controlled by distinct hydrogeochemical processes. No statistically significant linear correlation was observed between gross alpha activity and ^{222}Rn concentrations, indicating that the factors controlling ^{222}Rn occurrence were largely independent of those governing the distribution of dissolved alpha-emitting radionuclides in groundwater. The same was observed between gross beta and ^{222}Rn.

Gross alpha activity showed a moderate positive correlation with pH ($r = 0.493$; $p = 0.014$). This correlation suggests tha the mobility of alpha-emitting radionuclides is influenced by pH-dependent processes, possibly by adsorption/desorption reactions and changes in aqueous speciation. A plausible mechanism is that as groundwater pH increases, bicarbonate (HCO_3^-) and carbonate (CO_3^{2-}) concentrations generally increase, promoting the formation of highly stable and soluble uranyl carbonate complexes that enhance uranium mobility. Concurrently, the increasing alkalinity alters the surface charge of clay minerals and iron (oxyhydr)oxides, reducing the adsorption affinity of uranium and other alpha-emitting radionuclides. Consequently, previously sorbed radionuclides are desorbed from mineral surfaces and released into the aqueous phase, resulting in elevated alpha activity in groundwater.

Gross beta activity showed significant positive correlations with bicarbonate ($r = 0.514$; $p = 0.010$) and EC ($r = 0.547$; $p = 0.006$), both indicators of groundwater evolution and water-rock interaction. This suggests that beta-emitting radionuclides became more abundant as groundwater acquired dissolved ions through mineral weathering and prolonged contact with aquifer materials. This is consistent with the geochemical behavior of ^{210}Pb or ^{228}Ra (Jobbágy et al. 2010; Avwiri et al. 2016; Szabo et al. 2012; Matthews et al. 2018; Faraj et al. 2020).

The absence of significant correlations between ^{222}Rn activity and pH, bicarbonate, electrical conductivity, gross alpha, and gross beta activities indicate that dissolved radon is not primarily controlled by aqueous geochemical processes. As a chemically inert noble gas, ^{222}Rn does not undergo adsorption, complexation, or redox reactions in groundwater. Instead, its occurrence is governed by physical processes, including alpha recoil from the decay of ^{226}Ra, diffusion through pore spaces, emanation from mineral grains into groundwater, and accumulation during groundwater residence. The significant inverse relationship between ^{222}Rn and tritium ($r = -0.559$, $p = 0.004$) further supports this interpretation, indicating that older groundwater generally contains higher radon concentrations due to prolonged contact with radium-bearing aquifer materials (Assefa 2025).

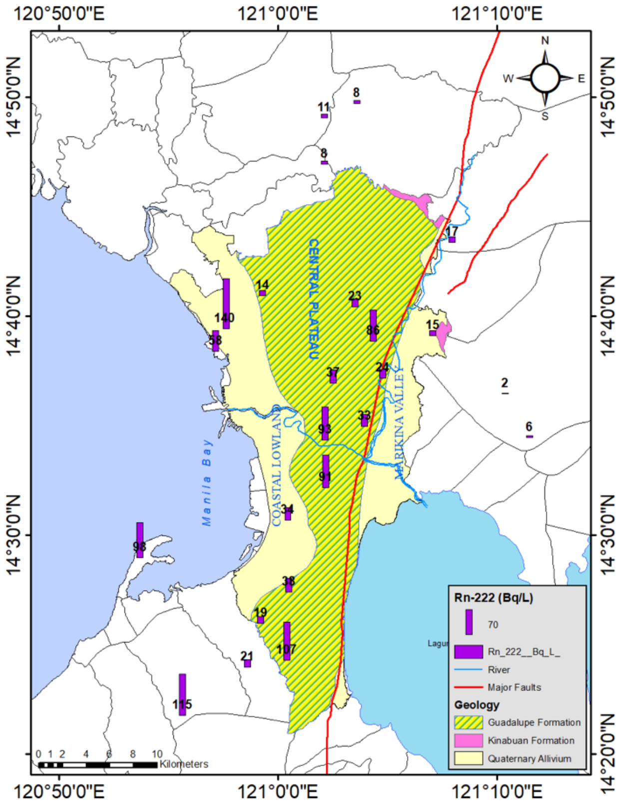

Figure 4: Spatial distribution of measured ^{222}Rn activity concentrations in groundwater samples.

Table 4: Comparison of the ^{222}Rn activity concentrations determined in groundwater samples with those reported in other countries.

Location	^{222}Rn activity concentration (Bq/L)		References
	Mean	Range	
Yerevan, Armenia	3.78	<LLD – 11.4	Pyuskyulyan et al. 2024
Dongpo, Hunan, China	10.47	1.29 – 31.31	Tan et al. 2019
Shimoga district, Karnataka, India	31.42	6.44 – 87.02	Shilpa et al. 2017
Dadri, India	33	17 – 68	Kumar et al. 2022
Campania region, Italy	9.71	1.00 – 37.23	Iannone et al. 2024
Calabria region, Italy	–	7.4 – 164	Caridi et al. 2023
Baling, Malaysia	5.7	1.9 – 11.9	Ahmad et al. 2018
Batangas, Philippines	16.84	4 – 51	Cadungog et al. 2025
Metro Manila, Philippines	47	2 – 140	This study
Makkah, Saudi Arabia	2.851	0.426 – 18.628	Hassan and Almatani 2022
Extremadura Region, Spain	98	0.15 – 1,200	Galán Lopez et al. 2004
Gezira State, Sudan	7.68	1.55 – 18.38	Elzain et al. 2024
Edu, Kwara, North-central Nigeria	24.16	21.59 – 27.93	Ajibola et al. 2021
Morocco	52.99	0.36 – 577.1	Tairi et al. 2024

Table 5: Pearson correlation analysis

	Gross Alpha (Bq/L)	Gross Beta (Bq/L)	Rn-222 (Bq/L)
Gross Alpha (Bq/L)	1		
Gross Beta (Bq/L)	-0.003 (p=0.99)	1	
Rn-222 (Bq/L)	0.104 (p=0.63)	0.020 (p=0.93)	1
Bicarbonate	0.281 (p=0.18)	0.514 (p=0.010)	0.124 (p=0.57)
Conductivity	0.400 (p=0.052)	0.547 (p=0.006)	0.197 (p=0.36)
pH	0.493 (p=0.014)	-0.033 (p=0.88)	0.106 (p=0.623)
Tritium	-0.046 (p=0.83)	-0.275 (p=0.19)	-0.559 (p=0.004)

Evaluation of the annual effective dose from groundwater ingestion

The specific radionuclides contributing to gross alpha and gross beta activities were not directly identified in this study. For conservative estimation, gross alpha activity was assumed to be represented by ^{226}Ra, as previous studies have shown that it contributes substantially to the ingestion dose (Damla et al. 2006). Gross beta was assumed to be represented by ^{210}Pb, which possesses relatively higher age-dependent ingestion dose coefficients than ^{40}K (Pintilie et al. 2018). It was further assumed that groundwater was consumed directly at the source without storage or treatment. This assumption represents a conservative exposure scenario.

The annual effective dose from ingestion (AED_{ing}) of ^{226}Ra, ^{210}Pb, and ^{222}Rn was evaluated for infants, children, and adults (Figure 5; Table 6). Mean ^{226}Ra ingestion doses were relatively low across all age groups (0.055, 0.022, and 0.016 mSv y^{-1} for infants, children, and adults, respectively), and no sample exceeded the WHO individual dose criterion (IDC) or screening level of 0.1 mSv y^{-1}.

Table 6: The annual effective doses due to the ingestion of radionuclides in groundwater

Radionuclides	Infant (mSv/y)		Child (mSv/y)		Adult (mSv/y)	
	Mean	Range	Mean	Range	Mean	Range
Ra-226	0.055 ± 0.042	0.020 – 0.127	0.022 ± 0.017	0.008 – 0.050	0.016 ± 0.012	0.006 – 0.037
Rn-222	0.480 ± 0.434	0.021 – 1.470	0.320 ± 0.289	0.014 – 0.980	0.334 ± 0.302	0.015 – 1.022
Pb-210	0.641 ± 0.626	0.178 – 2.268	0.338 ± 0.331	0.094 – 1.197	0.256 ± 0.250	0.071 – 0.907
Total	**1.177 ± 0.773**	**0.277 – 3.424**	**0.681 ± 0.445**	**0.139 – 1.933**	**0.606 ± 0.397**	**0.108 – 1.659**

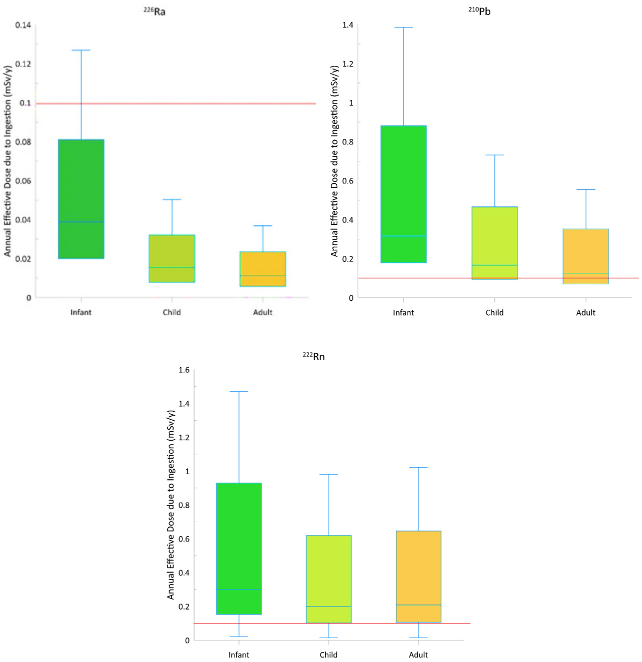

Figure 5: Annual effective doses due to ingestion (AED_{ing}) of (a)Radium-226, (b) Lead-210, and (c) Radon-222 in groundwater samples. The red line represents the WHO individual dose criterion or screening level of 0.1 mSv/y.

In contrast, ^{210}Pb contributed substantially to the ingestion dose. Mean ^{210}Pb doses reached 0.641 mSv/y in infants, 0.338 mSv/y in children, and 0.256 mSv/y in adults, all exceeding the IDC. ^{222}Rn was also a dominant contributor to ingestion dose, with mean doses of 0.480, 0.320, and 0.334 mSv/y for infants, children, and adults, respectively.

Total AED_{ing} values ranged from 0.277–3.424 mSv/y (mean: 1.177 mSv y^{-1}) for infants, 0.139–1.933 mSv/y (mean: 0.681 mSv/y) for children, and 0.108–1.659 mSv/y (mean: 0.606 mSv y^{-1}) for adults. The calculated total AED_{ing} exceeded the IDC in all samples, with several samples also exceeding 1 mSv y^{-1}, the recommended annual effective dose limit for members of the general public. These estimates are indicative and should be interpreted as conservative screening-level assessments rather than definitive measures of radiological risk.

Infants consistently received higher ingestion doses than children and adults because of their greater water intake relative to body mass and their higher age-dependent ingestion dose coefficients (Bem et al. 2014). Enhanced skeletal uptake of ^{226}Ra during periods of active bone growth further increases internal radiation burden among younger age groups (Muth and Glöbel 1983; Kawamura et al. 1991; Bronzovic and Marovic 2005).

Overall, alpha- and beta-emitting radionuclides each contributed approximately 50% of the total annual effective dose from ingestion. Despite their comparable contributions to the total dose, alpha-emitting radionuclides are radiologically more significant because alpha particles have a radiation weighting factor of 20, compared with 1 for beta particles, reflecting their much greater ionization density and biological effectiveness following internal exposure (ICRP 2007). These findings underscore the importance of considering not only radionuclide activity concentrations but also radiation weighting factors when evaluating the potential health risks associated with groundwater consumption.

Evaluation of the annual effective dose from inhalation of ^{222}Rn released into indoor air

In addition to ingestion, the inhalation pathway associated with ^{222}Rn degassing during domestic water use was evaluated (Table 7). In all age groups, ingestion remained the dominant exposure pathway, while inhalation and radon dissolved in blood contributed comparatively smaller fractions than ingestion (Figure 6).

Table 7: Total annual effective dose (mSv/y) from radon in drinking water.

Sample Code	AED_{ing} (mSv/y)			AED_{inh} (mSv/y)	$AED_{Rn,di}$ (mSv/y)	AED to Stomach and Lungs (mSv/y)				Total AED due to ^{222}Rn (mSv/y)		
						Stomach			Lungs			
	Infant	Child	Adult			Infant	Child	Adult		Infant	Child	Adult
PHI/MM/01	0.399	0.266	0.277	0.096	0.005	0.048	0.032	0.033	0.011	0.499	0.366	0.378
PHI/MM/02	0.200	0.133	0.139	0.048	0.002	0.024	0.016	0.017	0.006	0.250	0.183	0.189
PHI/MM/03	0.242	0.161	0.168	0.058	0.003	0.029	0.019	0.02	0.007	0.302	0.222	0.229
PHI/MM/04	0.903	0.602	0.628	0.217	0.010	0.108	0.072	0.075	0.026	1.130	0.829	0.855
PHI/MM/05	0.252	0.168	0.175	0.060	0.003	0.030	0.02	0.021	0.007	0.315	0.231	0.239
PHI/MM/06	0.158	0.105	0.110	0.038	0.002	0.019	0.013	0.013	0.005	0.197	0.145	0.149
PHI/MM/07	0.063	0.042	0.044	0.015	0.001	0.008	0.005	0.005	0.002	0.079	0.058	0.060
PHI/MM/08	0.021	0.014	0.015	0.005	0.000	0.003	0.002	0.002	0.001	0.026	0.019	0.020
PHI/MM/09	0.357	0.238	0.248	0.086	0.004	0.043	0.029	0.03	0.010	0.447	0.328	0.338
PHI/MM/10	0.084	0.056	0.058	0.020	0.001	0.010	0.007	0.007	0.002	0.105	0.077	0.080
PHI/MM/11	0.147	0.098	0.102	0.035	0.002	0.018	0.012	0.012	0.004	0.184	0.135	0.139
PHI/MM/12	1.124	0.749	0.781	0.270	0.013	0.135	0.09	0.094	0.032	1.406	1.031	1.063
PHI/MM/13	1.208	0.805	0.840	0.290	0.014	0.145	0.097	0.101	0.035	1.511	1.108	1.143
PHI/MM/14	0.084	0.056	0.058	0.020	0.001	0.010	0.007	0.007	0.002	0.105	0.077	0.080
PHI/MM/15	0.116	0.077	0.080	0.028	0.001	0.014	0.009	0.010	0.003	0.145	0.106	0.109
PHI/MM/16	0.221	0.147	0.153	0.053	0.002	0.026	0.018	0.018	0.006	0.276	0.202	0.209
PHI/MM/17	1.029	0.686	0.715	0.247	0.012	0.123	0.082	0.086	0.030	1.288	0.945	0.974
PHI/MM/18	0.179	0.119	0.124	0.043	0.002	0.021	0.014	0.015	0.005	0.223	0.164	0.169
PHI/MM/19	0.347	0.231	0.241	0.083	0.004	0.042	0.028	0.029	0.010	0.434	0.318	0.328
PHI/MM/20	0.389	0.259	0.27	0.093	0.004	0.047	0.031	0.032	0.011	0.486	0.357	0.368
PHI/MM/21	0.956	0.637	0.664	0.229	0.011	0.115	0.076	0.080	0.028	1.196	0.877	0.904
PHI/MM/22	0.977	0.651	0.679	0.234	0.011	0.117	0.078	0.081	0.028	1.222	0.896	0.924
PHI/MM/23	1.470	0.980	1.022	0.353	0.017	0.176	0.118	0.123	0.042	1.839	1.349	1.391
PHI/MM/24	0.609	0.406	0.423	0.146	0.007	0.073	0.049	0.051	0.018	0.762	0.559	0.576
Mean	**0.480 ± 0.434**	**0.320 ± 0.289**	**0.334 ± 0.302**	**0.115 ± 0.104**	**0.0054 ± 0.0049**	**0.058 ± 0.052**	**0.038 ± 0.035**	**0.040 ± 0.036**	**0.014 ± 0.013**	**0.601 ± 0.543**	**0.441 ± 0.398**	**0.455 ± 0.411**

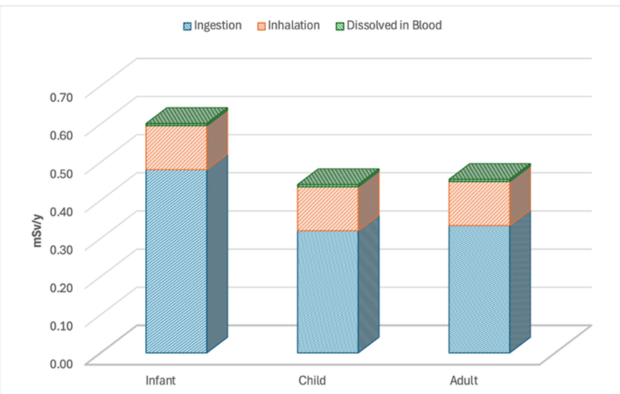

Figure 6: The contribution of doses to the total effective dose due to ^{222}Rn in infant, children, and adult age groups.

The annual effective dose from inhalation of radon released into indoor air ranged from 5 to 353 µSv/y, with a mean value of 155 ± 104 µSv/y. The dose associated with radon dissolved in blood was relatively minor, ranging from 0.2 to 16.7 µSv/y (mean: 5.4 ± 4.9 µSv/y).

Organ-specific doses indicate that ingestion primarily affected the stomach, while inhalation mainly affected the lungs (Shah et al. 2024). Estimated stomach doses ranged from 0.003 to 0.176 mSv/y in infants, 0.002 to 0.118 mSv/y in children, and 0.002 to 0.123 mSv/y in adults. Lung doses ranged from 0.001 to 0.042 mSv/y across all age groups.

Lifetime excess cancer risk and implications for groundwater management

Estimated total annual effective doses (AED_{tot}) from combined ingestion and inhalation pathways ranged from 0.282–3.683 mSv/y (mean: 1.298 ± 0.841) for infants, 0.144–2.192 mSv/y (mean: 0.801 ± 0.524) for children, and 0.114–1.918 mSv/y (mean: 0.727

± 0.487) for adults. These calculated doses indicate that the mean AED_{tot} values for all age groups exceeded the World Health Organization (WHO) individual dose criterion of 0.1 mSv/y. The estimated mean AED_{tot} values for children and adults remained below the recommended annual dose limit of 1 mSv/y for members of the general public, whereas the estimated mean value for infants was slightly above this benchmark. Nevertheless, the estimated mean AED_{tot} for all age groups remained below the global average annual effective dose from natural background radiation of 2.4 mSv/y. As these dose estimates are based on conservative assumptions regarding water consumption, equilibrium factors, and dose conversion coefficients, they should be regarded as indicative screening-level assessments rather than definitive measures of individual radiological risk.

The excess lifetime cancer risk (ELCR) estimates the incremental probability of developing cancer following lifetime exposure to low-dose ionizing radiation. This metric was calculated for adult male and female residents of Metro Manila (Table 8). The estimated ELCR was slightly higher for females than for males, reflecting the longer average life expectancy assumed in the risk model. For female residents, estimated ELCR values ranged from 4.60×10^{-4} to 7.76×10^{-3} (approximately 4–77 potential cases per 10,000 individuals), with a mean of 2.94×10^{-3} (approximately 29 potential cases per 10,000 individuals). For male residents, estimated ELCR values ranged from 4.10×10^{-4} to 6.93×10^{-3} (approximately 4–69 potential cases per 10,000 individuals), with a mean of 2.63×10^{-3} (approximately 26 potential cases per 10,000 individuals). The mean estimated ELCRs for both populations were above the reported global average value of 1.45×10^{-3} but remained below the recommended reference level of 3.75×10^{-3} (Oni et al. 2025). Although these estimates are subject to uncertainties associated with radionuclide attribution, water consumption patterns, and dose conversion factors, they suggest that chronic consumption of radionuclide-bearing groundwater could contribute to an increased probability of stochastic health effects, with relatively higher estimated risks for females because of their longer projected lifetime (Hançerlıoğullari et al. 2019; Salman et al. 2025). Accordingly, the ELCR values should be interpreted as conservative, screening-level indicators of potential long-term radiological risk rather than definitive predictions of cancer incidence.

Table 8: Excess lifetime cancer risk for male and female residents of Metro Manila due to ingestion of radionuclides in drinking water.

Sample Code	Location	AED_{tot} (mSv/y)	ELCR	
			Male	Female
PHI/MM/01	Parañaque City	0.77	0.00277	0.00311
PHI/MM/02	Las Piñas City	0.48	0.00173	0.00193
PHI/MM/03	Quezon City	0.34	0.00121	0.00136
PHI/MM/04	Quezon City	0.96	0.00348	0.00390
PHI/MM/05	Marikina City	0.50	0.00180	0.00202
PHI/MM/06	Marikina City	0.23	0.00084	0.00094
PHI/MM/07	Antipolo City, Rizal	0.15	0.00053	0.00060
PHI/MM/08	Antipolo City, Rizal	0.11	0.00041	0.00046
PHI/MM/09	Pasay City	0.65	0.00236	0.00264
PHI/MM/10	Caloocan City	0.16	0.00058	0.00065
PHI/MM/11	Valenzuela City	0.22	0.00079	0.00089
PHI/MM/12	Las Piñas City	1.15	0.00417	0.00467
PHI/MM/13	Imus, Cavite	1.24	0.00448	0.00501
PHI/MM/14	San Jose Del Monte, Bulacan	0.22	0.00078	0.00088
PHI/MM/15	San Jose Del Monte, Bulacan	0.47	0.00170	0.00190
PHI/MM/16	Bacoor, Cavite	1.12	0.00406	0.00454
PHI/MM/17	Cavite City, Cavite	1.92	0.00693	0.00776
PHI/MM/18	Rodriguez, Rizal	0.68	0.00245	0.00275
PHI/MM/19	Pasig City	0.74	0.00266	0.00298
PHI/MM/20	Quezon City	0.68	0.00244	0.00274
PHI/MM/21	Makati City	1.46	0.00529	0.00593
PHI/MM/22	Mandaluyong City	1.09	0.00393	0.00440
PHI/MM/23	Malabon City	1.47	0.00531	0.00594
PHI/MM/24	Navotas City	0.65	0.00236	0.00265
Mean ± SD		**0.727 ± 0.487**	**0.00263 ± 0.00176**	**0.00294 ± 0.00197**

The increasing reliance on groundwater abstraction in Metro Manila following drought-induced water shortages underscores the need to incorporate radiological parameters into routine groundwater monitoring programs. Public communication regarding groundwater radiation hazards is particularly important for households with infants and children.

Mitigation measures such as aeration, storage prior to distribution, or blending with low-radon water sources could substantially reduce exposure, especially in wells with elevated ^{222}Rn concentrations (National Research Council 1999). Future work should include radionuclide-specific analyses and hydrogeochemical modeling to better constrain the radionuclide sources and transport mechanisms within the aquifer system.

CONCLUSION

This investigation provides the first publicly available systematic radiological profile of Metro Manila's groundwater resources, highlighting important links between hydrogeology, regulatory compliance, and public health. The results demonstrate that, while dissolved alpha-emitting radionuclides remain well within the national screening level, natural leaching of radionuclides from the volcanic deposits of the Guadalupe Formation contributes to elevated gross beta activity. Furthermore, prolonged groundwater–rock interaction promotes the accumulation of ^{222}Rn, resulting in concentrations exceeding the national screening level of 11 Bq/L in 19 of the 24 surveyed production wells. These findings highlight the dominant influence of local geology and groundwater residence time on the occurrence of naturally occurring radionuclides in the Metro Manila aquifer system.

The estimated total annual effective doses, particularly for infants and children, and the excess lifetime cancer risk estimates that exceeded global reference values in some cases indicate a potential for increased long-term stochastic health risks associated with prolonged consumption of untreated groundwater from these aquifers. However, these findings should be interpreted within the context of the conservative exposure assumptions adopted in this study and should not be construed as evidence of a direct or causal health effect. Rather, the estimated doses and cancer risks serve as screening-level indicators derived from standardized radiological risk-assessment models and are subject to uncertainties related to radionuclide attribution, exposure frequency and duration, age-specific consumption patterns, and dose-conversion factors. Accordingly, they should be interpreted as indicative of potential radiological concerns that warrant continued monitoring and more site-specific investigations, rather than as definitive measures or predictions of individual health risk. Nevertheless, the findings highlight the value of practical public health interventions, including routine radiological monitoring of groundwater resources, optimization of community-level aeration and storage practices to facilitate radon removal, and, where feasible, blending of high-radon groundwater with low-radon sources to reduce public exposure. Collectively, these results provide an important baseline for water resource managers and policymakers to guide future monitoring programs, refine risk assessments, and support the sustainable management of groundwater resources in the face of the region's growing dependence on them.

ACKNOWLEDGMENTS

This research was made possible through the collaboration of the National Water Resources Board (NWRB), which provided on-site support and invaluable assistance in sampling. This research did not receive any funding from local or international sources.

CONFLICT OF INTEREST

The authors declare that they have no competing interests related to this work. All financial and non-financial relationships and interests, direct or indirect, that could be perceived as influencing the work reported in this paper have been disclosed.

CONTRIBUTIONS OF INDIVIDUAL AUTHORS

Norman DS. Mendoza: Writing – review & editing, Data curation. **Jeff Darren G. Valdez:** Writing – review & editing, Data curation. **Raymond J. Sucgang:** Writing – review & editing. **Mylene G. Cayetano:** Writing – review & editing. **Charles Darwin T. Racadio:** Writing – original draft, Visualization, Validation, Software, Resources, Methodology, Formal analysis, Data curation, Conceptualization

REFERENCES

Ahmad N, ur Rehman J, Rafique M, Nassir T. Age-dependent annual effective dose estimations of ^{226}Ra, ^{232}Th, ^{40}K and ^{222}Rn from drinking water in Baling, Malaysia. Water Supply 2018; 18(1): 32-39 https://doi.org/10.2166/ws.2017.094

Ajibola TB, Orosun MM, Lawal WA, Akinyose FC, Salawu NB. Assessment of annual effective dose associated with radon in drinking water from gold and bismuth mining area of Edu, Kwara, North-central Nigeria. Pollution 2021; 7(1): 231-240. https://doi.org/10.22059/poll.2020.309470.892

Ali K, Matar ZS, Walther C, El-Din KS, Harb S, Kilany M, Moubark K. Radionuclide Distribution and Hydrochemical Controls in Groundwater of the Nile Valley, Upper Egypt: Health and Environmental Implications. Water 2025; 17(18): 2730. https://doi.org/10.3390/w17182730

Almasoud FI, Ababneh ZQ, Alanazi YJ, Khandaker MU, Sayyed MI. Assessment of radioactivity contents in bedrock groundwater samples from the northern region of Saudi Arabia. Chemosphere 2020; 242: 125181. https://doi.org/10.1016/j.chemosphere.2019.125181

American Public Health Association, American Water Works Association, Water Environment Federation. "Liquid Scintillation Method. (7500-Rn B.)" In Standard Methods for the Examination of Water and Wastewater. Edited by W. C. Lipps, E. B. Braun-Howland, and T. E. Baxter. 24th ed. Washington, DC: APHA Press, 2023.

Assefa NA. Analysis of ^{226}Ra content and ^{222}Rn exhalation rates in soil samples from Wukro, Tigray, using SSNTDs. F1000Res 2025; 14: 289. https://doi.org/10.12688/f1000research.160449.1

Avwiri GO, Osimobi JC, Ononugbo CP. Gross alpha and gross beta activity concentrations and committed effective dose due to intake of water in solid mineral producing areas of Enugu State, Nigeria. Int J Phys Appl 2016; 8(1): 33-43. https://doi.org/10.33545/26647575.2025.v7.i2e.215

Barbosa-Lorenzo R, Barros-Dios JM, Ruano-Ravina A. Radon and stomach cancer. Int J Epidemiol 2017; 46(2): 767-768. https://doi.org/10.1093/ije/dyx011

Bem H, Plota U, Staniszewska M, Bem EM, Mazurek D. Radon (^{222}Rn) in underground drinking water supplies of the Southern Greater Poland Region. J Radioanal Nucl Chem 2014; 299(3): 1307-1312. https://doi.org/10.1007/s10967-013-2912-1

[BFS] Bundesamt für Strahlenschutz, (2026) Ionizing Radiation Accessed at https://www.bfs.de/EN/topics/ion/environment/foodstuffs/introduction/introduction_node.html#:~:text=Foods%20of%20plant%20origin%20can,edible%20parts%20of%20the%20animals on March 16, 2026.

Bonotto DM. Gross alpha/beta radioactivity and radiation dose in thermal and non-thermal spas groundwaters. Heliyon 2019, 5(5): e01563. https://doi.org/10.1016/j.heliyon.2019.e01563

Bonotto DM, Bueno TO. The natural radioactivity in Guarani Aquifer Groundwater, Brazil. Appl Radiat Isot 2008; 66: 1507-1522. https://doi.org/10.1016/j.apradiso.2008.03.008

Bronzovic M, Marovic G. Age-dependent dose assessment of Ra-226 from bottled water intake. Health Phys 2005; 88(5): 480-485. https://doi.org/10.1097/01.hp.0000154007.12917.88

Cadungog DGE, Racadio CDT, Valdez JDG, Racho JMD, Mendoza NDS, Sucgang RJ. Radiological investigation of radon in groundwater around the active Taal Volcano (Philippines) and dose evaluation. Environ Geochem Health 2025; 47: 287. https://doi.org/10.1007/s10653-025-02610-w

Caridi F, Paladini G, D'Agostino M, Marguccio S, Belvedere A, Belmusto G, Stilo G, Majolino D, Venuti V. Radon-specific activity in drinking water and radiological health risk assessment: a case study. Appl Sci 2023; 13(17): 9660. https://doi.org/10.3390/app13179660

Cfarku F, Xhixha G, Bylyku E, Zdruli P, Mantovani F, Përpunja F, Callegari I, Guastaldi E, Xhixha Kaçeli M, Thoma H. A preliminary study of gross alpha/beta activity concentrations in drinking waters from Albania. J Radional Nucl Chem 2014; 301, 435-442. https://doi.org/10.1007/s10967-014-3142-x

Chen Z, Liu Z, Wang J, Zhou X, Du, J. Radon emission from soil gases in the active fault zones in the Capital of China and its environmental effects. Sci Rep 2018; 8: 16772. https://doi.org/10.1038/s41598-018-35262-1

Currie LA. Limits for qualitative detection and quantitative determination: application to radiochemistry. Anal Chem 1968; 40: 586–593. https://doi.org/10.1021/ac60259a007

Daag AS, Halasan OPC, Magnaye AAT, Grutas RN, Solidum Jr RU. Empirical correlation between Standard Penetration Resistance (SPT-N) and Shear Wave Velocity (Vs) for soils in Metro Manila, Philippines. Appl Sci 2022; 12(16): 8067. https://doi.org/10.3390/app12168067

Damla N, Cevik U, Karahan G, Kobya AI. Gross alpha and beta activities in tap water in eastern black sea region of Turkey. Chemosphere 2006; 62(37): 957-960. https://doi.org/10.1016/j.chemosphere.2005.05.051

Das B. Scenario of radon alpha activity level in natural drinking waters of different regions of eastern part of India: A review report. Indian J Sci Technol 2021; 14: 1189-1204. https://doi.org/10.17485/IJST/v14i15.46

de la Paz LR, Palattao MVB, Estacio JF, Ragiles SC. Seismic characteristics of the area around the Philippine Research Reactor (PRR-1). Quezon City, Philippines: Philippine Nuclear Research Institute, 1989: 6.

Dungca JR, Gozum NLC, Telan JAS, Torres VCF, Uytengsu TSY. Deep foundation reference for Metro Manila, Philippines. Int J GEOMATE 2018; 14(45): 16-21. https://doi.org/10.21660/2018.45.7135

Eidy M, Regina AC, Tishkowski K. Radon Toxicity. In: Statpearls [Internet]. Treasure Island (FL): StatPearls Publishing, 2024. Available from: https://www.ncbi.nlm.nih.gov/books/NBK562321/

Elzain AEA, Shady R, Yagob AA. Assessment of environmental radioactivity concentration and effective dose rates from radon gas exposure from water samples in Gezira State, Sudan. Radioprot 2024, 59(3): 235-245. https://doi.org/10.1051/radiopro/2024018

Ezzulddin SK, Mansour HH. Assessment of radon exposure in Erbil drinking water resources. ZANCO J Pure Appl Sci 2017; 29(4): 184-194. http://dx.doi.org/10.21271/ZJPAS.29.s4.22

Faraj TK, Ragab A, El Alfy M. Geochemical and hydrogeological factors influencing high levels of radium contamination in groundwater in arid regions. Environ Res 2020; 184(3): 109303. https://doi.org/10.1016/j.envres.2020.109303

Forte M, Rusconi R, Cazzaniga MT, Sgorbati G. The measurement of radioactivity in Italian drinking water. Microchem J 2007; 85(1): 98-102. https://doi.org/10.1016/j.microc.2006.03.004

Galán López M, Martín Sánchez A, Gómez Escobar V. Estimates of the dose due to 222Rn concentrations in water. Radiat Prot Dos 2004, 111(1): 3-7. https://doi.org/10.1093/rpd/nch350

Gervacio FC. The geology, structures and landscape development of Manila and suburbs. The Philippine Geologist 1968; 21(4): 178-192.

Hançerlıoğullari A, Turhan Ş, Kurnaz A. Evaluation of the Lifetime Cancer Risk Due to Natural Radioactivity in Tap Water Consumed in Nevşehir Province, Turkey. BEU J Sci 2019; 8: 46-48. https://doi.org/10.17798/bitlisfen.633417

Hassan RA, Almatani TU. Assessment of radon levels in groundwater in the city of Makkah, KSA. J Umm Al-qura Univ Appl Sci 2022; 8: 2-7. https://doi.org/10.1007/s43994-022-00004-7

Ho PL, Hung LD, Minh VT, Chinh DV, Tranh TT, Tao CV. Simultaneous determination of gross alpha/beta activities in groundwater for ingestion effective dose and its associated public health risk prevention. Sci Rep 2020, 10: 4299. https://doi.org/10.1038/s41598-020-61203-y

Hornung RW, Reed LD. Estimation of average concentration in the presence of nondetectable values. Appl Occup Environ Hyg 1990; 5(1): 46-51. https://doi.org/10.1080/1047322X.1990.10389587

Howard B. Environmental Pathways of Radionuclides to Animal Products in Different Farming and Harvesting Systems. In: Naletoski I, Luckins AG, Viljoen G, eds. Nuclear and Radiological Emergencies in Animal Production Systems, Preparedness, Response and Recovery [Internet]. Berlin, DE: Springer, 2021: Chapter 5. https://doi.org/10.1007/978-3-662-63021-1_5

Iannone A, Albanese S, Guarino A, Ambrosino M, Germano G, De Tullio G, Cicchella D. Variation of total alpha and beta activities and Rn-222 concentrations in the water supply system of an Italian volcanic region: How safe is tap water for human consumption?. J Hazard Mater 2024; 470: 134229. https://doi.org/10.1016/j.jhazmat.2024.134229

[IARC] International Agency for Research on Cancer. Man-made mineral fibres and radon IARC Monographs on the evaluation of carcinogenic risks to humans, Vol 43. Lyon: IARC, 1988.

[ICRP] International Commission on Radiological Protection. The 2007 Recommendations of the International Commission of Radiological Protection. Annals of the ICRP, 37(2-4). ICRP Publication 103. Oxford, United Kingdom: Pergamon Press, 2007.

ICRP] International Commission on Radiological Protection. Compendium of Dose Coefficients based on ICRP Publication 60. Annals of the ICRP, 41 Supplement 1. ICRP Publication 119. London, United Kingdom: Elsevier Ltd., 2012.

Isinkaye MO, OlaOlorun OA, Chandrasekaran A, Adekeye AS, Dada TE, Tamilarasi A, Sathishm V, Khandaker MU, Almujally A, Tamam N, Suleiman A. Quantification of radiological hazards associated with natural radionuclides in soil, granite and charnockite rocks at selected fields in Ekiti State, Nigeria.

Heliyon 2023; 9(11): e22451. https://doi.org/10.1016/j.heliyon.2023.e22451

Janković MM, Todorović DJ, Todorović NA, Nikolov J. Natural radionuclides in drinking waters in Serbia. Appl Radiat Isot 2012; 70: 2703-2710. https://doi.org/10.1016/j.apradiso.2012.08.013

[JICA] Japan International Cooperation Agency. Establishment of graphic information base project of National Capital Region, Republic of the Philippines. Makati City, Philippines: JICA, 1989.

[JICA] Japan International Cooperation Agency. Study for the groundwater development in Metro Manila .Volume 2 Main Report.Makati City, Philippines: JICA, 1992.

[JICA] Japan International Cooperation Agency. The Study of Masterplan on High Standard Highway Network Development in the Republic of The Philippines. Makati City, Philippines: JICA, 2010.

Jobbágy V, Wätjen U, Meresova J. Current status of gross alpha/beta activity analysis in water samples: a short overview of methods. J Radioanal Nucl Chem 2010; 286: 393-399. https://doi.org/10.1007/s10967-010-0709-z

Jobbágy V, Kávási N, Dombovári C, Gyöngyösi C, Kovács T. Gross alpha and beta activity concentrations in spring waters in Balaton Upland, Hungary. Radiat Meas 2011; 46(1): 159-163. https://doi.org/10.1016/j.radmeas.2010.08.004

Kashkinbayev Y, Kazhiyakhmetova B, Altaeva N, Bakhtin M, Tarlykov P, Saifulina E, Aumalikova M, Ibrayeva D, Bolatov A. Radon Exposure and Cancer Risk: Assessing Genetic and Protein Markers in Affected Populations. Biology 2025; 14(5): 506. https://doi.org/10.3390/biology14050506

Kawamura H, Yamamoto M, Igarashi Y, Shiraishi K, Ueno K. Naturally occurring ^{226}Ra concentrations in bone at various ages and alpha doses in adults. Health Phys 1991; 61(5): 615-622. https://doi.org/10.1097/00004032-199111000-00004

Keith S, Doyle JR, Harper C, Mumtaz C, Tarrago O, Wohlers DW, Diamond GL, Citra M, Barber LE. Toxicological Profile for Radon. Atlanta, Georgia, USA: Agency for Toxic Substances and Disease Registry, Public Health Service, US Department of Health and Human Services, 2012.

Kumar M, Kumar P, Agrawal A, Sahoo BK. Radon concentration measurement and effective dose assessment in drinking groundwater for the adult population in the surrounding area of a thermal power plant. J Water Health 2022, 20(3); 551-559. https://doi.org/10.2166/wh.2022.265

Lantz PM, Mendez D, Philbert MA. Radon, Smoking, and Lung Cancer: The Need to Refocus Radon Control Policy. Am J Public Health 2013; 103(3): 443-447. https://doi.org/10.2105/AJPH.2012.300926

Liu Y, Fu C, Li Y, Xu W, Huang Z, Xu Y. Uncovering hidden dangers in urban housing: Sources of indoor radon and associated health risks. J Environ Manage 2025; 387: 125899. https://doi.org/10.1016/j.jenvman.2025.125899

Livesay RJ, Blessinger CS, Guzzardo TF, Hausladen PA. Rain-induced increase in background radiation detected by Radiation Portal Monitors. J Environ Radioact 2014; 137: 137-141. https://doi.org/10.1016/j.jenvrad.2014.07.010

Lubin JH, Colt JS, Camann D, Davis S, Cerhan JR, Severson RK, Bernstein L, Hartge P. Epidemiologic evaluation of measurement data in the presence of detection limits. Environ Health Perspect 2004; 112(17): 1691-1696. https://doi.org/10.1289/ehp.7199

Luna RAC, Quebral RD, Gargullo JMB, Leobrera KJR, Selda PAY, Marasigan ED, Armario MJP, Baniquett MP. Geotechnical and geophysical characterization of the Guadalupe Tuff Formation – the regional bedrock of Metro Manila, Philippines. In: Rahman R, Jaksa M, eds. Proceedings of the 20th International Conference on Soil Mechanics and Geotechnical Engineering. Sydney, Australia: Australian Geomechanics Society, 2022.

Mabry J, Romeo N, Kainz G, Copia L, Masuda H, Matsumoto T. Development of the ^{3}He mass spectrometric low-level tritium analytical facility at the IAEA. J Anal At Spectrom 2022; 37; 2502.

Matthews M, Gotkowitz M, Ginder-Vogel, M. Effect of geochemical conditions on radium mobility in discrete intervals within the Midwestern Cambrian-Ordovician aquifer system. Appl Geochem 2018; 97: 238-246. https://doi.org/10.1016/j.apgeochem.2018.08.025

Mbembe SM, Mbembe BA, Maya J, Mohamadou LL, Boubakari M. Preliminary Studies on ^{222}Rn Concentration in Groundwater of Yaounde, Cameroon. J Appl Math Phys 2021; 9: 1423-1433. https://doi.org/10.4236/jamp.2021.97095

Miura H, Midorikawa S, Fujimoto K, Pacheco BM, Yamanaka H. Earthquake damage estimation in Metro Manila, Philippines, based on seismic performance of buildings evaluation by local experts' judgements. Soil Dyn Earthq Eng 2008; 28: 764-777. https://doi.org/10.1016/j.soildyn.2007.10.011

Mohammed AA, Abdulhussein SA, Falih AH, Abd Alameer ZS. Assessment of radon-222 levels in groundwater and drinking water and evaluation of health and environmental risks in Al-Baitha and surrounding areas southeast of Baghdad. Arab J Geosci 2026; 19: 44. https://doi.org/10.1007/s12517-026-12456-w

Muth H, Glöbel B. Age dependent concentration of ^{226}Ra in human bone and some transfer factors from diet to human tissues. Health Phys 1983; 44(1): 113-121. https://doi.org/10.1097/00004032-198306001-00009

National Research Council (US) Committee on Risk Assessment of Exposure to Radon in Drinking Water. C Water Mitigation Techniques In: Risk Assessment of Radon in Drinking Water. Washington, D.C., U.S.A.: National Academies Press, 1999.

[NWRB] National Water Resource Board. Water Resources Assessment for Prioritized Critical Areas (Phase 1) Final Report (Metro Manila). Manila, Philippines: CEST Inc., 2004.

Ofori JA, Addison ECK, Subaar C, Ashai EA, Asamoah E. The impact of radionuclides on water consumption in some water samples in the Ashanti Region, Ghana. J Water Health 2025; 23(8): 907-922. https://doi.org/10.2166/wh.2025.200

Oni EA, Olajide TA, Oladejo OP, Suleman KO, Salaudeen SA, Adewumi HI, Owojori AA, Oyero OP, Sunmonu LA, Egbeyale GB. Spatial distribution of natural radionuclides and its radiological impact in a fractured sedimentary zone, Nupe basin, north-central Nigeria. Discov Geosci 2025; 3: 157. https://doi.org/10.1007/s44288-025-00274-8

[PAGASA] Philippine Atmospheric Geophysical and Astronomical Services Administration. State of the 2022 Philippine Climate. Pasig City, Metro Manila: The Oscar M Lopez Center for Climate Change Adaptation and Disaster Risk Management Foundation Inc., 2024.

Pintilie V, Ene A, Georgescu LP, Moraru L, Iticescu C. Measurements of gross alpha and beta activity in drinking water from Galati Region. Rom Rep Phys 2016; 68(3): 1208-1220.

Pintilie V, Ene A, Georgescu L, Moraru DI, Pintilie A. Determination of Gross Alpha Gross Beta and Natural Radionuclides (^{210}Po, ^{21}0Pb, ^{238}U, ^{232}Th, and ^{40}K) Activity Concentrations in Bread and Their Contribution to the Effective Dose. Rom J Phys 2018; 63(1-2): 801.

[PNSDW] Philippine National Standards for Drinking Water. Manila, Philippines: Department of Health, 2017. Available at https://www.fda.gov.ph/wp-content/uploads/2020/10/Administrative-Order-No.-2017-0010.pdf

[PSA] Philippine Statistics Authority. Population and Housing. In: 2020 Philippine Statistical Yearbook. Manila, Philippines: PSA, 2020. Available at https://psa.gov.ph/system/files/psy/2020%20PSY_final.pdf

Pyuskyulyan K, Pipoyan D, Hovhannisyan S, Beglaryan M, Movsisyan N, Belyaeva O. Assessing radon hazard in drinking water: A comprehensive approach integrating deterministic and probabilistic methods with water consumption routines. Sci Tot Environ 2024; 949: 175217. https://doi.org/10.1016/j.scitotenv.2024.175217

Rimando RE, Knuepfer PLK. Neotectonics of the Marikina Valley fault system (MVFS) and tectonic framework of structures in northern and central Luzon, Philippines. Tectonophysics 2006; 415(1-7): 17-38. https://doi.org/10.1016/j.tecto.2005.11.009

Salman AY, Kadhim SA, Hussain HM, Sharrad FI. Assessing the Excess Lifetime Cancer Risk from Water in the Euphrates River, Najaf, Iraq. Health Phys 2025; 29(4): 245-255. https://doi.org/10.1097/HP.0000000000001959

Sang C, An W, Sørensen PB, Han M, Hong Y, Yang M. Gross alpha and beta measurements in drinkable water from seven major geographical regions of China and the associated cancer risks. Ecotoxicol Environ Saf 2025; 208: 111728. https://doi.org/10.1016/j.ecoenv.2020.111728

Schwela D, Kotzias D. Pollution Air Indoor. In:) Wexler P, ed. Encyclopedia of Toxicology. Second Edition. Cambridge, Massachusetts, United States: Academic Press, 2005: 475-489.

Shah SSA, Asif AR, Ilahi M, Haroon H, Islam I, Qadir A, Nisar I, Sani MMU, Iqbal R, Rahman MHU, Arslan M, Alwahibi MS, Elshikh MS, Ditta A. Geographical distribution of radon and associated health risks in drinking water samples collected from the Mulazai area of Peshawar, Pakistan. Sci Rep 2024; 14(1): 6042. https://doi.org/10.1038/s41598-024-55017-5

Shilpa GM, Anandaram BN, Mohankumari TL. Measurement of ^{222}Rn concentration in drinking water in the environs of Tirthahalli taluk, Karnataka, India. J Radiat Res Appl Sci 2017; 10: 262-268. https://doi.org/10.1016/j.jrras.2017.05.007

Shouop CJG, Fogue R, Ateba JFB, Fokou M, Simo A, Moyo MN. ^{222}Rn and ^{220}Rn levels in drinking water, the related health implications, and influencing environmental parameters in the volcanic area of Nkongsamba, Cameroon. Appl Environ Soil Sci 2026; 2717927. https://doi.org/10.1155/aess/2717927

Sucgang RJ, Pabroa PCB, Mendoza NDS, Racho JMD, Castaneda SS. Method development for radon measurement and simultaneous determination of gross alpha and gross beta activities in water by liquid scintillation counting for compliance testing of samples to the Philippine National Standards for drinking water. Vienna, Austria: International Nuclear Information System, International Atomic Energy Agency, 2012.

Sucgang RJ, Pabroa PCB, Castañeda SS. Method validation for the in-house developed procedure for Liquid Scintillation Spectroscopy for the determination of gross alpha and gross beta activities in water. Asia Life Sci 2023; 31 (1 & 2): 157-162.

Szabo Z, dePaul VT, Fischer JM, Kraemer TF, Jacobsen E. Occurrence and geochemistry of radium in water from principal drinking-water aquifer systems of the United States. Appl Geochem 2012; 27(3): 729-752. https://doi.org/10.1016/j.apgeochem.2011.11.002

Tairi A, Bouchaou L, Hssaisoune M, Bentahar Z, Mostafa MYA. Exploring radon risk in groundwater: insights from few investigated areas in Morocco. Environ Earth Sci 2024; 83: 396. https://doi.org/10.1007/s12665-024-11704-0

Tan W, Li Y, Tan K, Xie Y, Han S, Wan P. Distribution of radon and risk assessment of its radiation dose in groundwater drinking for village people nearby the W-polymetallic metallogenic district at Dongpo in southern Hunan province, China. Appl Radiat Isot 2019; 151: 39-45. https://doi.org/10.1016/j.apradiso.2019.05.008

Tulchinsky TH, Varavikova EA, Cohen MJ. Chapter 9 - Environmental and occupational health In: Tulchinsky TH, Varavikova EA, Cohen M J, eds. The New Public Health. Fourth Edition. Cambridge, Massachusetts, U.S.A: Academic Press, 2023.

Turhan Ş, Özçitak E, Taşkin H, Varinlioğlu A. Determination of natural radioactivity by gross alpha and beta measurements in ground water samples. Water Res 2013; 47: 3103-3108. http://dx.doi.org/10.1016/j.watres.2013.03.03

[UNSCEAR] United Nations Scientific Committee on the Effects of Atomic Radiation. Sources and Effects of Ionizing Radiation, Volume I: Sources. UNSCEAR 2000 Report. New York, U.S.A.: United Nations, 2000.

[UNSCEAR] United Nations Scientific Committee on the Effects of Atomic Radiation. Sources and Effects of Ionizing Radiation, Volume I: Sources. UNSCEAR 2008 Report. New York, U.S.A.: United Nations, 2008.

[WHO] World Health Organization. Guidelines for Drinking-water Quality: Fourth Edition. Geneva, Switzerland: WHO, 2011.

[WHO] World Health Organization. Guidelines for Drinking-water Quality: Fourth Edition Incorporating the First and Second Addenda. Geneva, Switzerland: WHO, 2022.

[WHO] World Health Organization. Philippine Data. Accessed at https://data.who.int/countries/608 on June 29, 2026.